

## An approach for double-frequency signals generation and analogue transmission with high inter-modulation distortion suppression

Jiang Wei<sup>1,2</sup>, Zhao Shanghong<sup>1</sup>, Qin Weize<sup>2</sup>, Tan Qinggui<sup>2</sup>, Liang Dong<sup>2</sup>

(1. Information and Navigation College, Air Force Engineering University, Xi'an 710077, China;  
2. National Key Laboratory of Science and Technology on Space Microwave, Xi'an 710100, China)

**Abstract:** An approach of double-frequency signal generation and analogue transmission with high inter-modulation distortion suppression was described, which can be widely used for Radio Over Fiber(ROF) system. The approach was mainly based on a Dual-Parallel Mach-Zehnder modulator (DPMZM) and two electrical phase shifters. By adjusting the three biases of the DPMZM, double-frequency signals with high inter-modulation distortion suppression were generated. On the same structure, by adjusting bias of MZM2, which is the sub-modulator of DPMZM, and controlling the electrical drive voltages on the electrodes of MZM2, an analog photonic link with high IMD3 (third-order inter-modulation distortion) suppression was realized. From tests, the double-frequency signals with inter-modulation distortion suppression of approximately 30 dB and the analog photonic link with complete IMD3 suppression were validated and proved. The approach reduces the difficulty, complexity, and costs of ROF system, while increasing the stability of ROF system. Experimental results for IMD3 suppression are well matched with the analysis ones.

**Key words:** distortion suppression; DPMZM; IMD3

**CLC number:** TN29      **Document code:** A      **DOI:** 10.3788/IRLA201847.S122002

## 一种具有高交调抑制比的倍频信号产生及模拟信号传输方法

蒋 炜<sup>1,2</sup>, 赵尚弘<sup>1</sup>, 秦伟泽<sup>2</sup>, 谭庆贵<sup>2</sup>, 梁 栋<sup>2</sup>

(1. 空间工程大学 信息导航学院, 陕西 西安 710077;  
2. 空间微波技术国家级重点实验室, 陕西 西安 710100)

**摘 要:** 基于 DPMZM 和两个电移相器, 文中给出了一种具有高交调抑制比的倍频信号产生及模拟信号传输方法, 该方法可广泛应用于 ROF 系统中。通过调整 DPMZM 的直流偏置工作点和电移相器相位, 可生成高交调失真抑制比的倍频信号。基于同一结构, 仅调整 DPMZM 中一个子调制器的直流工作点就可以实现高线性模拟信号传输。实验结果表明, 所生成的倍频信号的交调失真比可达 30 dB 以上; 所构建的高线性模拟信号传输链路可完全抑制三阶交调失真分量。该方法在降低 ROF 系统难度和复杂度的同时, 大大提高了系统稳定性。实验结果与理论分析结果相吻合。

**关键词:** 失真抑制; 双平行马赫-增德尔调制器; 三阶交调

收稿日期: 2018-03-05; 修订日期: 2018-05-14

基金项目: 国家自然科学基金(61231012); 国家预研基金(614241105010717)

作者简介: 蒋炜(1979-), 女, 高级工程师, 主要从事激光通信及星载微波光子通信转发方面的研究。Email: tsingh504@163.com

导师简介: 赵尚弘(1964-), 男, 教授, 博士生导师, 博士, 主要从事微波光子学及空间光通信网络方面的研究。Email: zhaoshangh@aliyun.com

## 0 Introduction

With the development of global information socialization, the objective of UNS –Ubiquitous Network Society is raised and has become a main focus of national informatization strategy for many countries. With this objective, it is a high-demanding in offering such heterogeneous broadband wireless services as cellular phone, wireless LAN (local area network) and terrestrial digital broadcasting services etc., in wireless networks<sup>[1-5]</sup>. The development of such information technology has opened a new era for ROF applications.

Due to the fact that ROF system takes the advantages of both optical fiber and wireless technologies, it is considered a unique platform for the integration of heterogeneous wireless services. Figure 1 shows the architecture of typical multi-service hybrid ROF system. First, RF signals are modulated on

optical carrier.

The central office (CO) then allocates wireless resources and routes signals. Afterwards, the optical line terminal (OLT) in CO sends signals to base stations(BSs) over fiber. Finally, the modulated optical signals from CO are received by a BS, and get demodulated to RF signals, before they are transmitted to end users by wireless equipments.

Due to the reason that multi-service hybrid fiber ROF system needs to carry heterogeneous wireless signals, mm-wave(millimeter wave) signals which can carry huge amount of data is needed in the CO. In addition, an analogue transmission link with multi-signals is also needed in the CO. Optical mm-wave generation methods have attracted great interest for ROF system, thanks to numerous advantages including low loss, high bandwidth, simple structure and immunity to electromagnetic interference. In recent years, some schemes on mm-wave signal generation with different methods have been reported<sup>[6-10]</sup>.

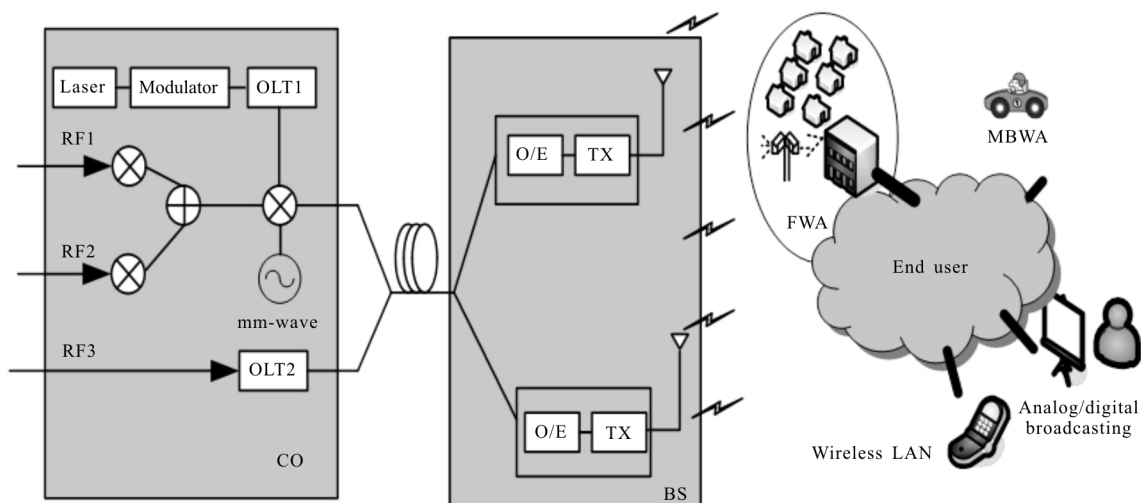


Fig.1 Architecture of typical multi-service hybrid ROF system

In Ref. [6], a new approach to generate optical carrier suppression mm-wave signal is proposed. However, the limitation with this approach is that it generates single mm-wave signal only and the structure is complicated. In Ref. [7-8], other new approaches to generate sextupling-frequency optical mm-wave are proposed. However, there's a strict

requirement on the level of RF (radio frequency) signal power, which changes along with the change of half-wave voltage of MZM (Mach-Zehnder modulator). In Ref. [9-10], a photonic technique, which is based on DPMZM, for MMW-UWB (mm-wave ultra-wideband) signal generation is raised. As the method works in a DSB (double-sideband)

modulation mode, it suffers from dispersion-induced power fading when the optical signals transmit over standard SMF (single mode fiber); and also, it is suitable for short distance transmission systems only. In Ref. [11], a frequency octupling based on DP-QPSK is analyzed and experimentally demonstrated. Unfortunately, it can only generate single mm-wave and the operation is complicated.

In addition, there are heterogeneous RF signals in CO, and an analog transmission link with multi-signals is needed. Herein, SFDR (spurious free dynamic range) is an important parameter for signal transmission, and it is closely related to inter-modulation distortions (mainly IMD3) that are introduced by the nonlinearity of the external modulators. To eliminate the IMD3 and improve the SFDR of the analog photonic link, some schemes based on phase modulator<sup>[13-14]</sup>, DD-MZM (Dual-drive MZM)<sup>[15-16]</sup> and DPMZM<sup>[17-19]</sup> have been studied in the past few decades. Both the schematics in Ref. [13] and [14] employ DSP aided coherent detection to realize linearity. However, the digital demodulation part needs highly-coherent detector, which increases the complexity of signal demodulation. In Ref. [15-16], analog photonic link with DD-MZM is proposed. In Ref. [15], it needs very accurate differential delays and multi-parameter controllers, which increase the complexity and cost. In Ref. [16], to suppress IMD3, except for coherent detection, additional polarization devices with precise polarization alignment are needed, such as polarization combiner, polarization splitter and linear polarizer. In Ref. [17], it needs rigorous optical power split controller and high quality coherent optical local oscillation. In Ref. [18], it is too hard to balance the symmetrically single sideband modulation, which increases the complexity of the system, while decreases its stability greatly. In addition, based on bi-directional use of a polarization modulator in a Sagnac loop, a microwave photonic link is demonstrated in Ref. [19], although a 16 dB improvement of SFDR is achieved, it needs optical amplification and accurate

polarization controller.

All the methods above are from studies of either mm-wave signal generation of single RF signal, or IMD3 suppression of analog photonic link, but there's no single method to generate multi RF signals or analog photonic link with high IMD3 suppression on the same structure. In practice, because multi RF signals are usually available in ROF system, inter-modulation and harmonic distortions are inevitable in the process of mm-wave signal generation. This no doubt increases the difficulties in realizing multiple-frequency microwave signals frequency doubling. In addition, in order to reduce the complexity of CO system construction and associated cost, it is hoped that both multi RF signal IMD3 suppression and high quality transmission of multiband signals can be achieved by changing minimum parameters.

In this paper, an innovative approach to generate double-frequency signals with high inter-modulation distortion suppression and analogue signal transmission is proposed. The approach is mainly based on a DPMZM and two electrical phase shifters. Two sinusoidal electrical signals are sent to DPMZM simultaneously. Among which, one electrical signal modulated on two MZMs of DPMZM is out of phase. By optimizing the three biases of the DPMZM, OCS (optical carrier suppression) is achieved in DPMZM. Thus, double-frequency microwave signals with high inter-modulation distortion suppression can be generated. In addition, by adjusting the biases of MZM2 to quadrature point, and controlling the electrical drive voltages on the electrodes of MZM2, an analog photonic link with complete IMD3 suppression can be realized too. Without any filter and other optical processors, the proposed approach combines double-frequency mm-wave signals generation and analog photonic link with IMD3 suppression. The proposed approach has the advantages of more than one mm-wave signal generation, high inter-modulation suppression, huge bandwidth and high flexibility.

### 1 Principle

A design of the proposed approach is shown in Fig.2. The scheme consists of a LS (laser source), two microwave sources, two phase shifters, a DPMZM composed of three submodulators, and a PD

(Photodiode). A light wave emitted from a laser source denoted as  $E_{in}(t)$ , is sent to DPMZM. To calculate double-frequency signals in the usual manner, we use microwave sources to provide two sinusoidal electrical signals. The frequencies of electrical signals are  $\omega_1$  and  $\omega_2$  respectively, and electrical signal with  $\omega_2$  modulated on the two MZMs of DPMZM is out of phase.

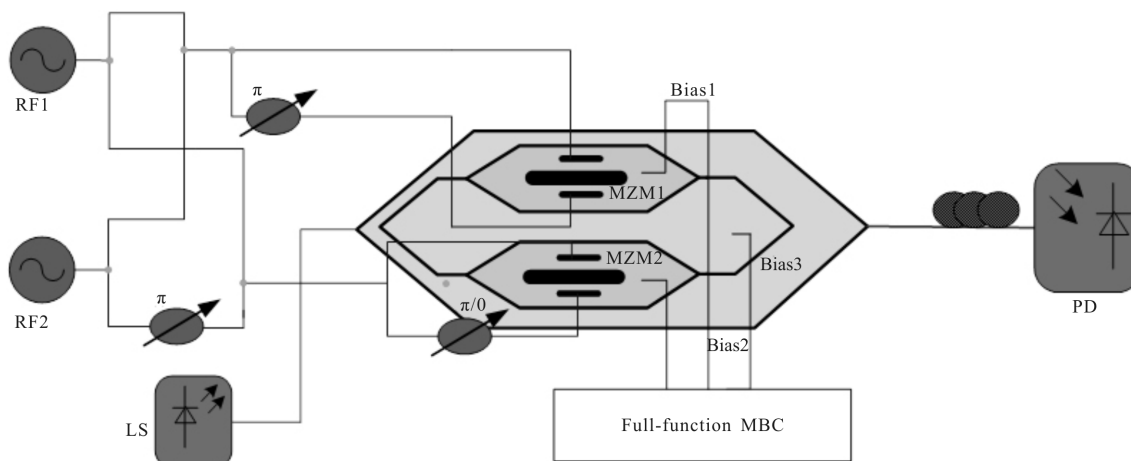


Fig.2 A design of the proposed optical double-frequency signal generation with high inter-modulation distortion suppression

Here, the electrical signals with  $\omega_1$  and  $\omega_2$  are sent to MZM1. The electrical signal with  $\omega_1$  and the electrical signal after  $\pi$  phase shift with  $\omega_2$  are sent to MZM2. When MZM1 and MZM2 operate at push-pull mode, OCS is achieved in DPMZM.

The light wave launched to the DPMZM is denoted as  $E_{in}(t)=E_0 \exp(j\omega_c t)$ ,  $\omega_c$  is the frequency of optical carrier, and the power level of laser is denoted as  $P_{in}=E_{in}(t) \cdot E_{in}^*(t)$ . The output optical field of MZM1 usually follows the expression of:

$$E_{out1}(t)=\sqrt{2\alpha} / 2 \times [\gamma \times \exp(j\varphi_{1i}) + (1-\gamma) \times \exp(j\varphi_{2i})] E_{in}(t) \quad (1)$$

where  $\alpha$  is the insert loss of MZM1;  $\gamma$  is the splitting ratio and its value is 0.5.  $\varphi_{1i}$  and  $\varphi_{2i}$  are phase shift angles of MZM1;  $\varphi_{1i}=\pi V_{1i}(t)/V_\pi + V_{DC1i}$  ( $i=1,2$ ), and  $V_\pi$  is half-wave voltage of MZM1;  $V_{DC1i}$  is the DC bias voltage of MZM1. The drive voltages on the electrodes of MZM1 can be expressed as following:

$$V_{11}(t)=V_m(\cos\omega_1 t + \cos\omega_2 t) \quad (2)$$

$$V_{12}(t)=V_m[\cos(\omega_1 t + \pi) + \cos(\omega_2 t + \pi)] \quad (3)$$

In this approach, if the insert loss of MZM is ignored, the output optical field of MZM1 can be

shown as:

$$E_{out1}(t)=[\exp(j\pi V_{11}(t)/V_\pi) \times \exp(j0) + \exp(j\pi V_{12}(t)/V_\pi) \times \exp(-j\pi)] E_{in}(t) = [\exp(j \frac{\pi V_m}{V_\pi} \cos\omega_1 t) \times \exp(j \frac{\pi V_m}{V_\pi} \cos\omega_2 t) - \exp(-j \frac{\pi V_m}{V_\pi} \cos\omega_1 t) \times \exp(-j \frac{\pi V_m}{V_\pi} \cos\omega_2 t)] E_{in}(t) \quad (4)$$

Using Jacobi-Auger expansions and Eq. (4) can be expands as:

$$E_{out1}(t)=E_{in}(t) \sum_{p=-\infty}^{\infty} \sum_{q=-\infty}^{\infty} (j)^{p+q} J_p(m) J_q(m) \exp(j(p\omega_1 t + q\omega_2 t)) \times [1 - (-1)^{p+q}] = E_{in}(t) \cdot (2) \sum_{p=-\infty}^{\infty} \sum_{\substack{q=-\infty \\ p+q \neq \text{even}}}^{\infty} (j)^{p+q} J_p(m) J_q(m) \times \exp(j(p\omega_1 t + q\omega_2 t)) \quad (5)$$

where  $m = V_m/V_\pi$  represents the modulation index. Similarly, the drive voltages on the electrodes of MZM2 can be written as:

$$V_{21}(t)=V_m[\cos(\omega_1 t) + \cos(\omega_2 t + \pi)] \quad (6)$$

$$V_{22}(t)=V_m[\cos(\omega_1 t + \pi) + \cos(\omega_2 t)] \quad (7)$$

Assuming the performance parameters of MZM2 are the same as MZM1, the output optical field of

MZM2 is given by:

$$E_{out2}(t)=[\exp(j\pi V_{21}(t)/V_{\pi})\times \exp(j\times 0)+\exp(j\pi V_{22}(t)/V_{\pi})\times \exp(j\times \pi)]E_{in}(t)=E_{in}(t)\sum_{p=-\infty}^{\infty}\sum_{\substack{q=-\infty \\ p+q \neq \text{even}}}^{\infty}(j)^{p+q}J_p(m)J_q(m)[(-1)^q-(-1)^p]\exp(j(p\omega_1 t+q\omega_2 t)) \quad (8)$$

The output optical field of DPMZM can be expressed as  $E_{out}(t)=\sqrt{2}[E_{out1}(t)+E_{out2}(t)]/2$  by biasing the MZM3 to null point.

The output photocurrent after PD is given by  $I_{PD}(t)=\eta E_{out}(t) \cdot E_{out}^*(t)$ , where  $\eta$  is the responsivity of PD. Using Taylor series expansion to the third order in  $m$ , the following expression can be derived:

$$I_{PD}=\eta E_{out}(t) \cdot E_{out}^*(t)=\left\{\begin{aligned} &\eta[J_0^2(m)J_3^2(m)+J_1^2(m)J_2^2(m)+J_2^2(m)J_3^2(m)+ \\ &J_1^2(m)J_4^2(m)+J_1^2(m)J_2^2(m)+J_0^2(m)J_1^2(m)+ \\ &J_1^2(m)J_2^2(m)]+[4J_0(m)J_1(m)J_2(m)J_3(m)+ \\ &2J_1(m)J_2(m)J_3(m)J_4(m)] \cdot \\ &[\cos(4\omega_1 t-2\omega_2 t)+\cos(2\omega_1 t-4\omega_2 t)]+ \\ &[4J_0(m)J_1(m)J_2(m)J_3(m)+ \\ &2J_1(m)J_2(m)J_3(m)J_4(m)+ \\ &2J_0^2(m)J_1(m)J_3(m)+J_0(m)J_1^2(m)J_2(m)+ \\ &2J_0^2(m)J_1^2(m)+J_1(m)J_2^2(m)J_3(m)] \cdot \\ &[\cos(2\omega_1 t)+\cos(2\omega_2 t)]P_{in} \end{aligned}\right. \quad (9)$$

As shown in Eq. (9), by adjusting MZM1 and MZM2 to operate in push-pull mode, and controlling one of electrical signals modulated on the two MZMs of DPMZM out of phase, double-frequency signals with frequencies  $2\omega_1$  and  $2\omega_2$  are achieved simultaneously. In the meantime, the inter-modulation distortions of frequencies  $4\omega_1-2\omega_2$  and  $4\omega_2-2\omega_1$  are suppressed.

With the same structure, the bias of MZM2 is adjusted to quadrature point, and the electrical signals introduced in two modulation arms of MZM2 are the same. Using Taylor series expansion to the third order in  $m$ , the output photocurrent of DPMZM after PD is expressed as following<sup>[20]</sup>:

$$I_{PD}(t)=\frac{1}{2}\eta \cdot P_{in} \cdot \{(1-2m[\cos(\omega_1 t)+\cos(\omega_2 t)]+$$

$$m^2[1+\frac{1}{2}\cos(2\omega_1 t)+\frac{1}{2}\cos(2\omega_2 t)+\cos(\omega_1 t-\omega_2 t)+\cos(\omega_1 t+\omega_2 t)]+m^3[(\frac{1}{3}\cos(3\omega_1 t)+\cos(\omega_1 t)+\frac{1}{3}\cos(3\omega_2 t)+\cos(\omega_2 t))]\}+O(m^4) \quad (10)$$

From Eq. (10), it can be seen that IMD3 of frequencies  $2\omega_1-\omega_2$  and  $2\omega_2-\omega_1$  are eliminated completely, and an analog photonic link with complete IMD3 suppression is obtained.

As shown above, the electrical signal modulated on the two MZMs of DPMZM is out of phase. By adjusting MZM1 and MZM2 to operate in push-pull mode, double-frequency signals with high inter-modulation suppression are generated. By adjusting the bias of MZM2 to quadrature point, the analog photonic link with complete IMD3 suppression can be realized.

## 2 Experiment

To verify the validity of the proposed approach, the experimental setup as shown in Fig.2 is built. The LS emits the lightwave with central wavelength of 1550.12 nm, and with power of 16 dBm. The sinusoidal electrical signals with two tones at 7.9 GHz and 8 GHz respectively are produced by signal sources (Agilent E8257D). The integrated DPMZM (FUJITSU FTM7962EP) with 32 GHz bandwidth is used to modulate the sinusoidal electrical signals, the modulation loss of DPMZM is 5 dB, and the half-wave voltage of DPMZM is 5 V. According to the previous analysis, the sinusoidal electrical signals with two tones are divided into two paths. One is sent to the upper arm of DPMZM, and the other is sent to the lower arm of DPMZM after  $\pi$  phase shift, and the three biases of DPMZM are adjusted by using DC suppliers (GPC 6030D). The output signals of DPMZM are launched into a PD (Discovery Semiconductors DSC 20 H) to detect the electrical signals. The electrical spectrum is monitored by an electrical spectrum analyzer (R&S FSQ 40).

Figure 3 (a) shows the output electrical spectrum of a conventional approach based on DPMZM (in which the electrical signals are two tone electrical signals with the same amplitude, and the DC bias points are set to quadrature point). It describes the entire electrical spectrum of double-frequency signals and fundamental wave signals. The modulation distortions are very complicated and obvious. The inter-modulation distortions of double-frequency signals are suppressed by approximately 5 dB, and the IMD3 of input electrical signals are suppressed by approximately 9 dB. The entire electrical spectrum of the double-frequency signals from the proposed approach can be shown in Fig.3(b). It can be seen that the power difference between fundamental wave signals and double-frequency signals is 31 dB, and the inter-modulation distortions near the two double-frequency signals at 15.8 GHz and 16 GHz are suppressed.

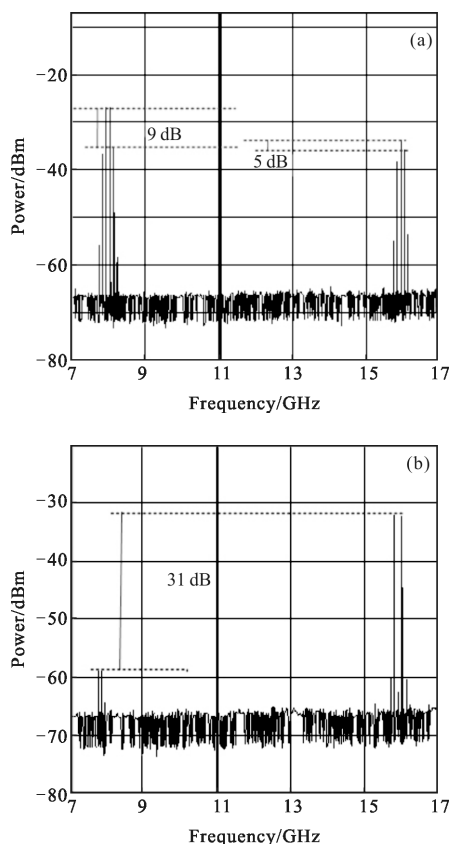


Fig.3 Entire electrical spectrum after PD with (a) conventional approach (b) the proposed approach

Figure 4 (a) shows the electrical spectrum of double-frequency signals with conventional approach, which is based on DPMZM. Figure 4 (b) shows the electrical spectrum of double-frequency signals with proposed approach. By comparing Fig.4(a) with Fig.4(b), it can be seen that only distortion components at 15.9GHz and 16.1 GHz exist (which is adjacent to the double-frequency signals at 15.8 GHz and 16 GHz), and the inter-modulation distortions are suppressed by approximately 30 dB in Fig.4(b).

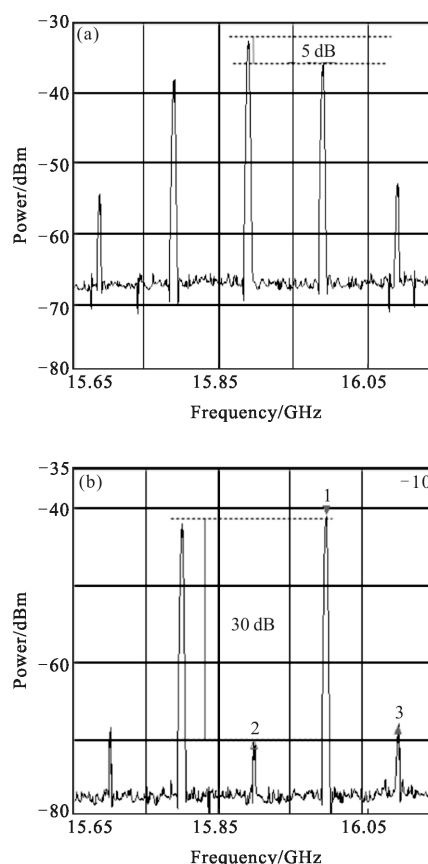


Fig.4 Electrical spectrum after PD of double-frequency signals generation (a) with conventional approach (b) with proposed approach

Figure 5(a) shows the inter-modulation components of fundamental wave signals in detail. Due to the nonlinearity of the DPMZM, the IMD3 at 7.8 GHz and 8.1 GHz is suppressed by approximately 9 dB only. In addition, other inter-modulation components of fundamental wave signals can be seen obviously, which has an influence on useful signals' transmission.

In Fig.5(b), no distortion components can be seen near the fundamental signals of 7.8 GHz and 8.1 GHz, and the IMD3 is lower than the noise floor with  $-90$  dBm level. That is to say, compared with conventional analog photonic link based on DPMZM, there is a great reduction of IMD3 in the proposed scheme, and IMD3 can be suppressed completely.

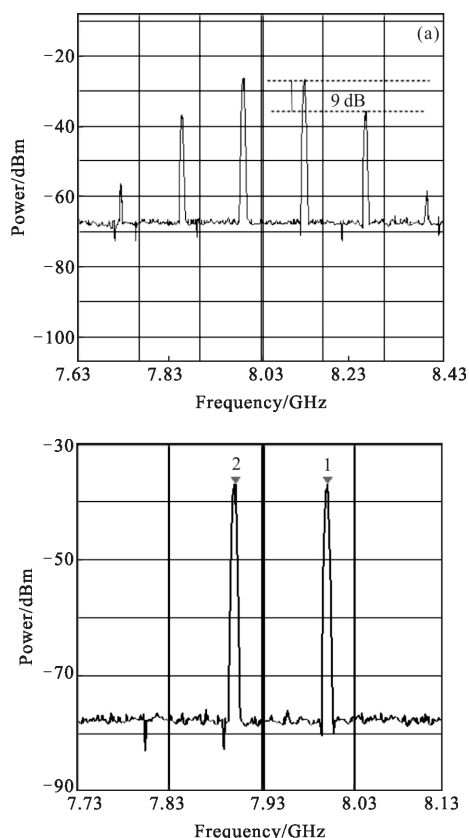


Fig.5 Electrical spectrum after PD of IMD3 suppression (a) conventional approach (b) proposed approach

### 3 Conclusion

In conclusion, an approach of double-frequency signals generation with high inter-modulation distortion suppression is proposed and demonstrated. By using mainly two phase shifters and optimizing the three biases of the DPMZM, double-frequency signals with two tones can be achieved; and the inter-modulation suppression is approximately 30 dB. On the same structure, by adjusting the biases of MZM2 to quadrature point and controlling the electrical drive voltages on the electrodes of MZM2 to the same, the

analog photonic link with complete IMD3 suppression can be realized. For the proposed approach without any digital processors and other optical processors, two microwave signals are generated, and the IMD3 of analog photonic link is completely suppressed. The proposed approach has the advantages of more than one microwave generation, high inter-modulation suppression, simple structure, long stabilization, and flexibility. Experiment results are in good accordance with the theoretical analysis results.

### References:

- [1] Maier M, Ghazisaidi N, Reisslein M. The audacity of fiber wireless (FiWi) networks [C]//ICST Int Conf Access Nets, 2008, 6: 16–35.
- [2] Chang G K, Liu C, Zhang L. Architecture and applications of a versatile small-cell, multi-service cloud radio access network using radio-over-fiber technologies [C]//IEEE International Conference on Communications (ICC), 2013, 51 (4): 879–883.
- [3] Gomes N J, Assimaopoulos P, Vieira L C, et al. Fiber link design considerations for cloud-radio access networks [C]// IEEE International Conference on Communications (ICC), 2014: 1109.
- [4] Ghazisaidi N, Scheutzow M, Maier M. Survivability analysis of next-generation passive optical networks and fiber-wireless access networks[J]. *IEEE Transactions on Reliability*, 2017, 60: 737–740.
- [5] Wake D, Nkansah A, Gomes N J. Radio over fiber link design for next generation wireless systems [J]. *J Lightw Technol*, 2010, 28: 2456–2464.
- [6] Shi P M, Yu S, Li Z K, et al. A novel frequency sextupling scheme for optical mm-wave generation utilizing an integrated dual-parallel Mach-Zehnder modulator [J]. *Optics Communications*, 2010, 283: 3667–3672.
- [7] Muthu K E, Raja A S. Frequency sextupling using single LN-MZM and 2.5 Gb/s ROF transmission [C]//IEEE Wispnet, 2016: 1842–1844.
- [8] Lu J, Dong Z, Liu J F, et al. Generation of a frequency sextupled optical millimeter wave with a suppressed central using one single-electrode modulator [J]. *Optical Fiber Technology*, 2014, 20: 533–536.
- [9] Li W, Zhu N H. Photonic MMW-UWB signal generation

- via DPMZM-based frequency up-conversion [J]. *IEEE Photonics Technology Letters*, 2013, 25: 1875-1877.
- [10] Sebastian Babiak, Astushi Kanno. Radio-over fiber photonic wireless bridge in the W-Band[C]//ICC, 2013, 25: 838-842.
- [11] Gao Y S, Wen A J, Jiang W, et al. Photonic microwave generation with frequency octupling based on a DP-QPSK modulator [J]. *IEEE Photonics Technology Letters*, 2015, 27: 2260-2263.
- [12] Liang D, Jiang W, Tan Q G, et al. A novel optical millimeter-wave signal generation approach to overcome chromatic dispersion[J]. *Optics Communications*, 2014, 320: 94-98.
- [13] Clar T R, O' Connor S R, Dennis M L. A phase-modulation I/Q demodulation microwave-to-digital photonic link [J]. *IEEE Trans Microw Theory Tech*, 2010, 58: 3039-3058.
- [14] Cui Y, Dai Y T, Yin F F, et al. Enhanced spurious-free dynamic range in intensity-modulated analog photonic link using digital post processing [J]. *IEEE Photonics Journal*, 2014, 6: 1-8.
- [15] Zhu Z H, Zhao S H, Tan Q G, et al. A linearized optical single-sideband modulation analog microwave photonic link using dual-parallel interferometers [J]. *IEEE Photonics Journal*, 2013, 5: 5501712.
- [16] Li X, Zhu Z H, Zhao S H. An intensity modulation and coherent balanced detection intersatellite microwave photonic link using polarization direction control [J]. *Optical & Laser Technology*, 2014, 56: 362-366.
- [17] Li S, Zheng X, Zhang H, et al. Highly linear radio-over-fiber system incorporating a single-drive dual-parallel Mach-Zehnder modulator [J]. *IEEE Photonics Technology Letters*, 2010, 24: 1775-1777.
- [18] Li J, Zhang Y C, Yu S, et al. Third-order intermodulation distortion elimination of microwave photonics link based on integrated dual-drive dual-parallel Mach-Zehnder modulator [J]. *Optics Express*, 2013, 38: 4285-4287.
- [19] Li W Z, Yao J P. Dynamic range improvement of a microwave photonic link based on bi-directional used of a polarization modulator in a Sagnac loop [J]. *Optics Express*, 2013, 13: 15692-15697.
- [20] Jiang W, Tan Q G, Qin W Z, et al. A linearization analog photonic link with high third-order intermodulation distortion suppression based on dual-parallel mach-zehnder modulator [J]. *IEEE Photonics Journal*, 2015, 3: 1-8.